Carbon films for photovoltaic devices

S.O. Rudchenko,[1] A.T. Pugachov,[1] V.E. Pukha,[1] V.V. Starikov,[1] S.N. Lavrynenko[1] and A.G. Mamalis[2, *]

[1] *National Technical University "KPI", Frunze St 21, 61002 Kharkov, Ukraine*
[2] *Project Centre for Nanotechnology and Advanced Engineering, NCSR "Demokritos", Athens, Greece*

The results of structural, mechanical and optical investigations of thin C_{60} and diamond-like carbon (DLC) films, considered as functional layers for photovoltaic converters, are presented. The absorption spectra are calculated and the optical band gaps of C_{60} and DLC films are determined based on experimentally obtained transmission and reflexion data. The multilayer system ITO/DLC/C_{60}/Al demonstrating a photovoltaic effect was synthesized and researched.

Keywords: absorption coefficient, band gap, current-voltage characteristics, diamond-like carbon film, fullerene

1. Introduction

The most efficient way to transform solar energy to electricity is by the use of semiconductor photovoltaic cells because it is a direct and single-step conversion of the energy [1].

Semiconductor materials with a band gap of 1–3 eV are the most suitable for manufacturing solar cells. There is a growing interest in carbon-based materials, including C_{60} and DLC films, for use in such systems (and in other electronic devices) [2].

It is expected that C_{60} films and systems using them will have ultrafast photo-induced charge transfer. Crystals and thin films of pure C_{60} demonstrate optical and electronic properties of n-type semiconductors and, at the same time, retain the peculiarities of their molecular structure. C_{60} thin films have high photoconductivity and their band gap is near to 1.6 eV: it is a parameter that can be changed depending on the molecular symmetry [3].

The amorphous carbon (a-C) known as DLC (diamond-like carbon) has significant amounts of sp^3-bonds. It demonstrates p-type conductivity, chemical inertness, mechanical durability and a wider band-gap in comparison with sp^2-bonded materials [4]. The DLC thin films are also interesting because of their combination of other attractive properties such as high hardness, low friction coefficient, IR transparency, chemical inertness, and the possibility to control the band-gap width and the conductivity type by the conditions of synthesis and doping [5]. The

* Corresponding author. E-mail: mamalis@ims.demokritos.gr

© 2013 Collegium Basilea

structure of these films and the sp^3:sp^2 bond ratio are determined by substrate temperature and deposition parameters (particle energy, flux density, precursor composition etc.). For room temperature deposition of DLC films employing different methods of ion generation (vacuum arc, laser evaporation etc.), the optimum energy should be about 100 eV [6].

The use of accelerated C_{60} ions as precursors allows the production of carbon films with some structural peculiarities. Variation in the ion energy and the substrate temperature leads to formation of DLC films, superhard conductive nanocomposites or nanographite structures [6]. Superhard DLC films, grown from C_{60} ions over a wide temperature range, have an electrical resistance two orders of magnitude lower than that of superhard DLC films deposited from a beam of accelerated carbon atoms under the same conditions [7].

Until now, carbon-based solar cells have been reported assembled using a C_{60}/Si heterojunction [8], an a-C/Si heterojunction [9, 10], n-C/p-C/p-Si [11], etc. This means that Si has been used as the substrate in all cases. The next step is to fabricate carbon solar cells on a glass substrate without using Si so that the advantage of the carbon solar cell becomes apparent.

Structural, mechanical, optical and electrical properties of both C_{60} and DLC films deposited from C_{60} ions are studied in the present work, with special emphasis on their functional properties as solar cells. The multilayer system ITO/DLC/C_{60}/Al, demonstrating a photovoltaic effect, was synthesized and its optical and electrical properties investigated.

2. Experimental

To obtain C_{60} and DLC films we used C_{60}-fullerene powder with a purity of 99.5% (NeoTechProduct, St Petersburg, Russia) as the initial material. The powder was purified by vacuum distillation before use.

The C_{60} films with a thickness of 1200 Å were obtained using thermal deposition in a vacuum chamber at a pressure $P \sim 1 \times 10^{-4}$ Pa and deposition rate 1 Å/s. DLC films were obtained using an ion beam with average C_{60} ion energy of $E_i = 5$ keV at a substrate temperature $T_s = 100$ °C, $P \sim 1 \times 10^{-4}$ Pa and deposition rate 1 Å/s. The films' thickness was 740 Å and they had p-type conductivity.

ITO films (In_2O_3 with 10% SnO_2) 0.4 μm thick were obtained by magnetron sputtering *in vacuo* on a glass substrate and were used as transparent conductive contacts.

For the fabrication of the carbon solar cell, the DLC and C_{60} films were consecutively grown on the ITO-coated glass substrates by the technique specified above. An Al thin film was deposited by thermal evaporation and used as the external electrode.

Optical properties of the films were investigated by an SF-26 double-beam spectrophotometer in the wavelength range $\lambda = 300$–1200 nm at room temperature. Optical transmission $T(\lambda)$ and reflectance $R(\lambda)$ spectra were measured. To decrease the effect of the glass substrate while recording $T(\lambda)$ spectra, a glass substrate without any film was placed in the reference beam. Reflectance spectra were measured using a PZO-2 accessory device providing double reflexion of light from the experimental sample compared with reflexion from the control sample.

Structural studies were carried out using a PEM-125K transmission electron microscope (TEM) having 0.2 nm point-to-point resolution. Samples for TEM measurements were deposited on the silicon substrate and prepared by chemical etching in a mixture of HF:HNO_3 = 1:10. Subsequently, the films were washed in deionized water and placed onto a copper grid.

The nanohardness and the elastic modulus were measured using a MTS G200 nanoindenter with a Berkovich diamond tip (radius $R < 20$ nm). A continuous depth-sensing indentation technique was used, which allows the recording of modulus and hardness as functions of penetration depth.

Raman measurements were carried out using a backscattering geometry with a JY LabRam HR instrument having a liquid nitrogen-cooled CCD detector. The spectra were collected using the 514.5 nm line of an argon ion laser.

The electrical resistivity of the synthesized films was estimated by the two-probe method. For the experimental multilayer systems of glass/ITO/DLC/C_{60}/Al both dark and loaded voltage–current characteristics were collected. Photovoltaic properties were measured under standard AM 1.5 illumination using a solar simulator placed on the glass side.

3. Results and discussion

The reflectance $R(\lambda)$ and transmission $T(\lambda)$ spectra of the C_{60} and DLC films are presented in Figs 1(a) and (b), respectively. The C_{60} films were characterized by high reflectance (~ 20%) in the infrared range, see curve 1 in Fig. 1(a), descending in the visible and UV ranges. The transmission spectra are given by curve 2. In the visible range the transmittance was 80–90 % and decreases close to the UV region. Some maxima and minima in the $R(\lambda)$ and $T(\lambda)$ curves were observed—they are artefacts associated with beam interference.

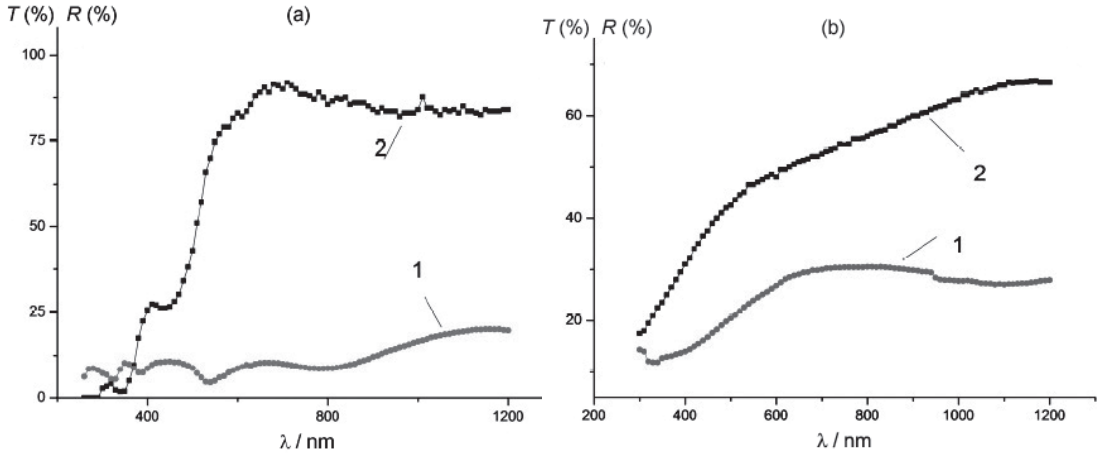

Figure 1. Reflectance (1) and transmittance (2) spectra: (a) C_{60} film; (b) DLC film.

The DLC films were also characterized by high reflectance (20–30%) in the infrared and visible range down to $\lambda \sim 500$ nm but dropping at shorter λ, see curve 1 in Fig. 1(b). Transmittance of DLC films in the infrared and visible spectral range was 55–65 %, decreasing in the ultraviolet range due to interband transitions, see curve 2.

The relatively high specular reflectances for all deposited films originate from their smooth surfaces. Interference peaks in the reflexion spectra of the films evidence their homogeneity over the substrate surface.

In order to estimate the optical width of the band gap E_g for thin C_{60} and DLC films, the following general equation was used, which is valid for direct band gap semiconductors:

$$\alpha\, h\nu = A\,[h\nu - E_g]^{1/2}, \tag{1}$$

where A is a constant depending on the effective masses of charge carriers in the material, $h\nu$ the photon energy and α the absorption coefficient.

Using equation (1), the linear part of the curve $(\alpha\, h\nu)^2$ vs $h\nu$ can be extrapolated onto the energy axis to estimate the energy gap of the semiconductor, see Fig. 2. Absorption coefficients of C_{60} and DLC films for calculating E_g were obtained taking into account the transmission and reflexion spectra using the following expression [12]:

$$\alpha = -\frac{1}{d}\ln\left(\frac{1}{R^2}\left(-\frac{(1-R)^2}{2T} + \sqrt{\frac{(1-R)^4}{4T^2} + R^2}\right)\right). \tag{2}$$

where R is the reflectance, T the transmittance and d the film thickness.

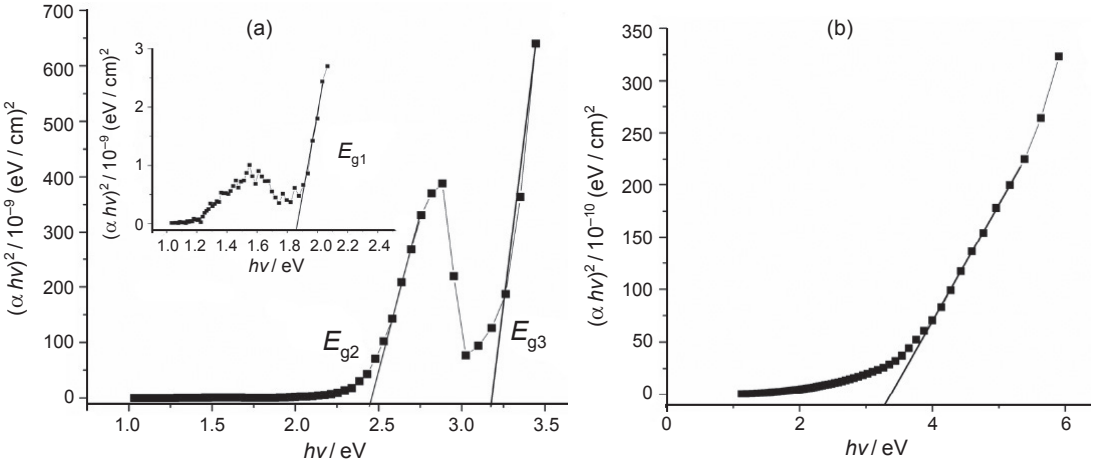

Figure 2. Estimation of optical band gap: (a) C_{60} film; (b) DLC film.

In Fig. 2, the absorption coefficient dependence $(\alpha\, h\nu)^2\ qua\, f(h\nu)$ curve, used to estimate band gaps of both the C_{60} and DLC films, is indicated. As can be seen, these dependencies in the region close to the red edge of absorption are approximated by straight lines, the intersections of which with the energy axis leads to determination of E_g.

The three characteristic energy transitions in the C_{60} film spectra are revealed in Fig. 2(a). Estimation of the transition energies yields the following values: $E_{g1} = 1.85$ eV; $E_{g2} = 2.45$ eV; and $E_{g3} = 3.2$ eV. The E_{g1} transition corresponds to the band gap of the C_{60} film [13, 14], which is polycrystalline with the face cubic centred (FCC) structure, see Fig. 3(a), and has photoresistive properties. The indices of the three strongest FCC reflexions are shown on the selected area electron diffractogram of the C_{60} film in Fig. 3(a).

According to our calculations, the band gap E_g of the DLC films was 3.25 eV, see Fig. 2(b). Electron diffraction and electron microscopy (EM) clearly demonstrate that the DLC films, obtained at a substrate temperature $T_s = 100$ °C and average ion energy $U_i = 5$ keV, have an amorphous structure and poorly developed surface relief. The contrast of the EM images is typical for amorphous films, and there are two halos in the diffraction pattern, with maxima characteristic of amorphous carbon, see Fig. (3b).

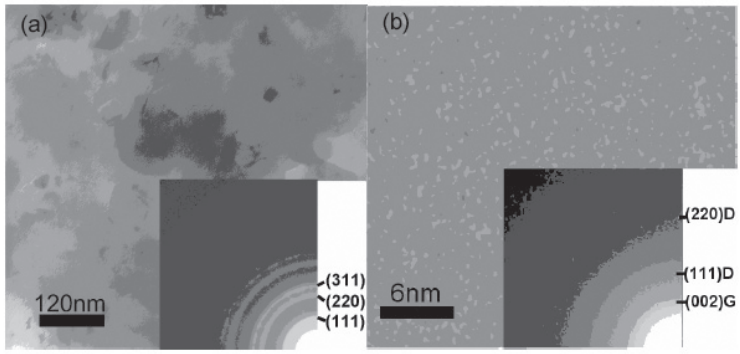

Figure 3. Representative transmission electron microscopy images and selected area electron diffraction (SAED) patterns of: (a) C_{60} film; and (b) DLC film obtained at U_i = 5 keV and T_s = 100 °C. The letters D and G on the SAED of the DLC indicated the most intense reflexions from the families of planes of diamond and graphite, respectively, calculated according to [16].

The fact that the films obtained at 100 °C and U_i = 5 keV had a diamond-like structure is confirmed by Raman spectroscopy, which showed a significant fraction of sp^3 bonds (~ 80%), and by nanoindentation of thick (~ 1 μm) films deposited on silicon. In Fig. 4, the Raman spectra for the samples deposited from ions with energies of ~ 5 keV are presented. Position and intensity of the D- and G-bands were determined by fitting with a Gaussian function and analysed on the basis of a phenomenological three-stage model (TSM) [15]; the derived parameters are presented in Table 1. The films deposited at 5 keV and T_s = 373 K have a low I(D)/I(G) ratio (~ 0.36) and the small downshift of the G-band indicates that the a-C film contains a large amount of sp^3 bonds (~ 80%, stage 3 of the TSM).

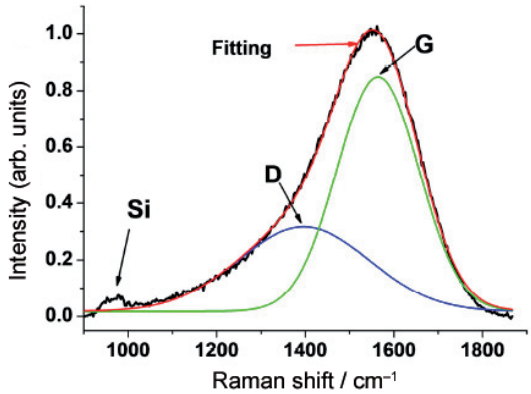

Figure 4. Results of fitting the broad band Raman spectrum between 900 and 1850 cm^{-1} with Gaussian functions (U_i = 5 keV, T_s = 373 K).

Table 1. Positions and intensity ratios of the D- and G-bands of the films deposited from C_{60} ions.

U_i / keV	T_s / K	G position / cm^{-1}	D position / cm^{-1}	I(D)/I(G)
5	373	1564	1396	0.36

The nanoindendation results for the DLC films are presented in Fig. 5, from which a Young's modulus of 336 GPa and a nanohardness of 46 GPa were derived [5]. It was thus demonstrated that the carbon films obtained from a C_{60} ion beam with an average energy of 5 keV were superhard films with diamond-like mechanical properties.

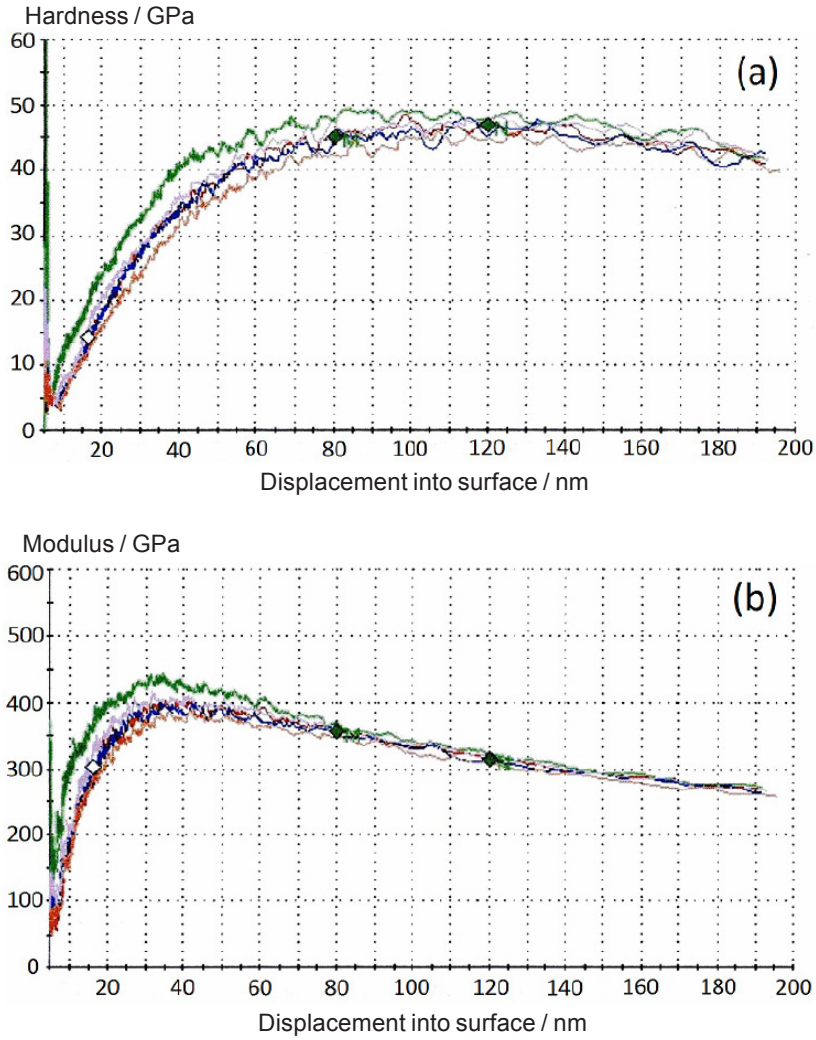

Figure 5. (a) Nanohardness and (b) Young's modulus of DLC films.

Based on the investigated films, the system glass/ITO/DLC/C_{60}/Al for demonstrating the photovoltaic effect has been synthesized and its dark current–voltage characteristic is presented in Fig. 6, the asymmetry of which indicates that in the contact zone of DLC–C_{60} layers, the p–n junction formed was capable of effectively separating the light-excited charge carriers. Because both the Al/a-C/ITO/glass and Al/C_{60}/ITO/glass systems show ohmic behaviour [17], it can be inferred that the observed dark current–voltage behaviour originates from the DLC/C_{60} p–n junction. This demonstrates the possibility of constructing photovoltaic cells based on such systems.

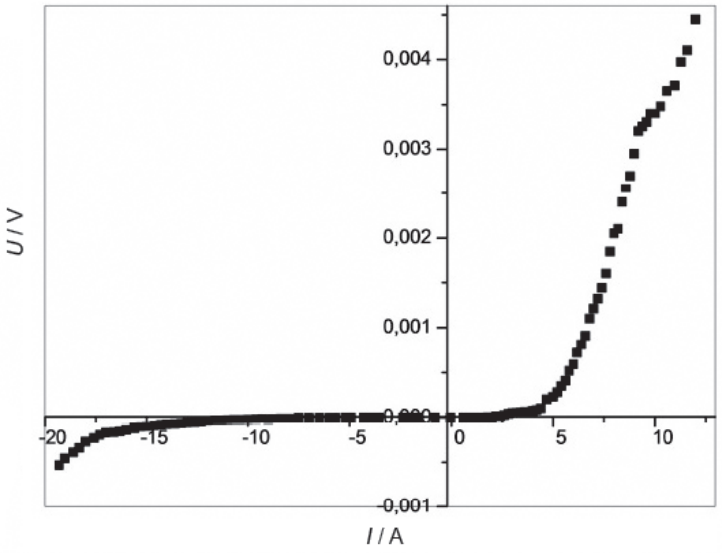

Figure 6. Dark current–voltage characteristic of the glass/ITO/DLC/C_{60}/Al system.

The load current–voltage characteristic of the glass/ITO/DLC/C_{60}/Al system is presented in Fig. 7. This curve allows the evaluation of both the maximum voltage generated and the maximum current determined by the internal resistance of the system. The maximum power generated is determined by the largest rectangle inscribable below the curve, which is used to quantify the efficiency of the photovoltaic cell (the "fill factor").

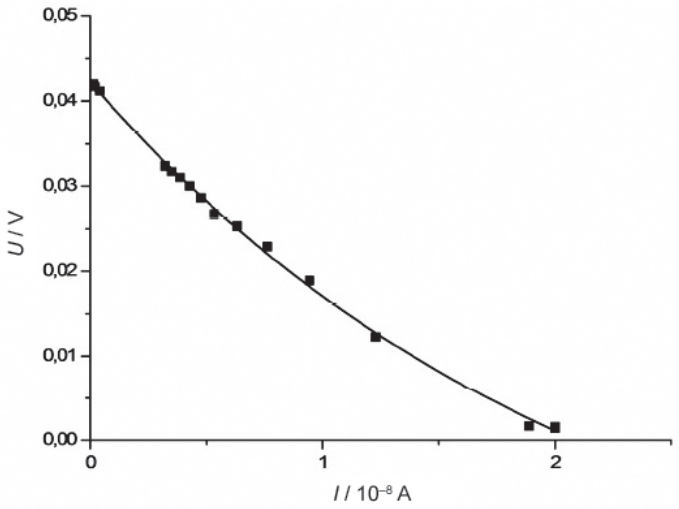

Figure 7. Load current–voltage characteristics of the glass/ITO/DLC/C_{60}/Al system.

The open circuit voltage was 0.0425 V and the short circuit current was 20 nA (at contact square 8 mm^2). Although the device performance is rather poor, the aim of this work is merely to demonstrate that an operating photovoltaic device made of carbon thin films is achievable.

4. Summary and conclusions

In the present work the transmission and reflexion of C_{60} and DLC films were quantified and the optical absorption and energy band gaps of the materials were estimated. Due to its wide band gap (~ 1.8 eV) the use of a photosensitive C_{60} layer as a base for the photoconverter is effective. Based on the studied films, the glass/ITO/DLC/C_{60}/Al system has been synthesized. In such a system, a p–n junction between the C_{60} and DLC layers is formed, which spacially redistributes (separates) the photogenerated charge. The combination of photosensitivity and p–n junction in this all-carbon system makes it interesting for the manufacture of photovoltaic cells.

References

1. Chopra, K.L. and Das, S.R. *Thin Film Solar Cells*. New York: Plenum Press (1983).
2. Faiman, D. Structure and optical properties of C_{60} thin films. *Thin Solid Films* **295** (1997) 283–286.
3. Katz, E. Fullerene thin films as photovoltaic materials. In: *Nanostructured Materials for Solar Energy Conversion* (ed. T. Soga), pp. 359–446. Elsevier (2006).
4. Milne, W. Electronic devices from diamond-like carbon. *Semicond. Sci. Technol.* **18** (2003) S81–S85.
5. Donnet, C. and Erdemir, A. (eds). *Tribology of Diamond-Like Carbon Films: Fundamentals and Applications*. New York: Springer (2008).
6. Pukha, V.E. and Pugachov, A.T. Synthesis, structure and properties of superhard nanostructured films deposited by the C_{60} ion beam. *J. Nanosci. Nanotechnol.* **12** (2012) 4762–4768.
7. Pukha, V.E., Zubarev, E.N., Drozdov, A.N., Pugachov, A.T., Jeong, S.H. and Nam, S.C. Growth of nanocomposite films from accelerated C_{60} ions. *J. Phys.* D **45** (2012) 335302 (9 pp.).
8. Narayanan, K.L. and Yamaguchi, M. Boron ion-implanted C_{60} heterojunction photovoltaic devices. *Appl. Phys. Lett.* **75** (1999) 2106–2107.
9. Krishna, K.M., Soga, T., Jimbo, T. and Umeno, M. A phosphorus-doped (n-type) carbon/boron-doped (p-type) silicon photo voltaic solar cell from a natural source. *Carbon* **37** (1999) 531–533.
10. Soga, T., Kokubu, T., Hayashi, Y. and Jimbo, T. Effect of rf power on the photovoltaic properties of boron-doped amorphous carbon/n-type silicon junction fabricated by plasma enhanced chemical vapor deposition. *Thin Solid Films* **482** (2005) 86 –89.
11. Krishna, K.M., Umeno, M., Nukaya, Y., Soga, T. and Jimbo T. Photovoltaic and spectral photoresponse characteristics of n-C/p-C solar cell on a p-silicon substrate. *Appl. Phys. Lett.* **77** (2000) 1472–1474.
12. Moss, T.S. and Balkanski, M. *Handbook on Semiconductors: Optical Properties*. Amsterdam: Elsevier (1994).
13. Mironov, G. I. and Murzashev, A.I. Energy spectrum of C_{60} fullerene. *Physics Solid State* **53** (2011) 2393–2397.
14. Sobolev, V.V. and Busygina, E.L. Electronic structure of C_{60} fullerite. *Physics Solid State* **41** (1999) 1025–1026.
15. Ferrari, A.C. and Robertson, J. Interpretation of Raman spectra of disordered and amorphous carbon. *Phys. Rev.* B **61** (2000) 14095–14107.
16. Powder Diffraction File. Inorganic Phases (ASTM). Swarthmore, Pennsylvania: International Center for Diffraction Data (ICDD) (1985).
17. Soga, T., Kondoh, T., Kishi, N. and Hayashi, Y. Photovoltaic properties of an amorphous carbon/fullerene junction. *Carbon* **60** (2013) 1–4.